KOKUYO セホ-50B

厚生労働科学研究費補助金
障害者対策総合研究事業

新規薬剤の生体内スクリーニングシステムの確立と網膜保護用デバイスの開発

平成２３年度　総括･分担研究報告書

研究代表者　阿部　俊明

平成２４（２０１２）年　５月

（２／２冊）

Journal of Controlled Release 151 (2011) 65–73

Contents lists available at ScienceDirect

Journal of Controlled Release

journal homepage: www.elsevier.com/locate/jconrel

NANOMEDICINE

Suppression of phagocytic cells in retinal disorders using amphiphilic poly (γ-glutamic acid) nanoparticles containing dexamethasone

Morin Ryu [a], Toru Nakazawa [a,*], Takami Akagi [b,c], Tatsuhide Tanaka [d], Ryou Watanabe [a], Masayuki Yasuda [a], Noriko Himori [a], Kazuichi Maruyama [e], Toshihide Yamashita [e], Toshiaki Abe [f], Mitsuru Akashi [b,c], Kohji Nishida [a,g]

[a] Department of Ophthalmology, Tohoku Graduate University School of Medicine, 1-1 Seiryo, Aoba, Sendai, Miyagi 980-8574, Japan
[b] Department of Applied Chemistry, Graduate School of Engineering, Osaka University, 2-1 Yamadaoka, Suita, Osaka 565-0871, Japan
[c] Japan Science and Technology Agency (JST), Core Research for Evolutional Science and Technology (CREST), Tokyo, Japan
[d] Department of Molecular Neuroscience, Graduate School of Medicine, Osaka University, 2-2 Yamadaoka, Suita, Osaka 565-0871, Japan
[e] Department of Ophthalmology, Kyoto Prefectural University of Medicine, 465 Kajiicho, Hirokojiagaru Kawaramachi-dori, Kamigyo-ku, Kyoto 602-084, Japan
[f] Division of Clinical Cell Therapy, Center for Advanced Medical Research and Development, United Centers for Advanced Research and Translational Medicine, Tohoku University Graduate School of Medicine, 2-1 Seiryo, Aoba, Sendai, Miyagi 980-8575, Japan
[g] Department of Ophthalmology, Osaka University School of Medicine, 2-2 Yamadaoka, Suita, Osaka 565-0871, Japan

ARTICLE INFO

Article history:
Received 16 August 2010
Accepted 26 November 2010
Available online 3 December 2010

Keywords:
Drug delivery
Nanoparticles
Neuroprotection
Cytokines
Monocyte recruitment
Microglia

ABSTRACT

To investigate the potential of nanoparticles (NPs) composed of poly(γ-glutamic acid) conjugated with L-phenylalanine (γ-PGA-Phe NPs) for the treatment of retinal diseases, γ-PGA-Phe NPs (200 nm) were tested with macrophages and microglia *in vitro* or by intravitreal administration into normal or pathological rat eyes. The anti-inflammatory effects of the NPs containing dexamethasone (DEX-NPs) were examined using qRT-PCR *in vitro* by counting activated microglia and Fluorogold-labeled retinal ganglion cells in the retinas under excitotoxicity or by counting TUNEL (+) photoreceptors in the detached retinas. The NPs were taken up efficiently by cultured macrophages or microglia. At day 7, 60–80% of the diffuse signal remained in the cytoplasm of these cells. In normal rat eyes, the NPs did not accumulate in the retinas and no inflammatory cells were recruited. Conversely, under pathological conditions, the NPs were localized in activated CD11b-positive cells in the retina. DEX-NPs suppressed the expression of TNFα and MCP-1 in cultured macrophages or microglia, the activation of microglia, the loss of retinal ganglion cells (RGCs) in excitotoxic retinas, and the number of TUNEL (+) photoreceptors in detached retinas. These data suggest that γ-PGA-Phe NPs can be a powerful tool for suppressing inflammatory cells in pathological conditions in the retina.

1. Introduction

Various delivery systems have the potential to deliver drugs over extended periods of time to specific cells without systemic complications [1–3]. Previously, drug-encapsulating polymeric microparticles (1–1000 μm) or nanoparticles (NPs: 10–1000 nm) were used for clinical applications to achieve sustained drug delivery, where the rate drug release depends on the rate of polymer degradation. Those polymers include polylactide (PLA) [4], poly(lactide-*co*-glycolid) (PLGA) [5–7], acrylic polymers, copolymers, hyaluronic acid derivatives, and alginates. Among the available biodegradable polymers, PLA [4] and PLGA are the most widely used, with degradation rates ranging from months to years [5–7] depending on the composition and molecular weight of the substance being released. However, major problems associated with PLA and PLGA polymers include the low encapsulation efficiency of highly water-soluble proteins and the instability during formulation, storage, and lyophilization of the NPs. Instability of the proteins also occurs during polymer degradation due to the accumulation of acidic monomers and the consequent generation of a low pH inside the biodegradable NPs.

Another important facet of drug delivery is the route of administration or carrier device. Prior studies have investigated eye drops or systemic administration with very small NPs (less than 20 nm) [8], subconjunctival administration [4], trans-scleral drug delivery with a trans-scleral depot containing the drugs [9], scleral implants [10], transcorneal or trans-scleral iontophoresis [11,12] and aerosol administration during surgery for vitrectomy [13]. These local application techniques helped to minimize systemic complications and provided higher concentrations of the drugs in the posterior portion of the eyes.

In this study, we used poly(γ-glutamic acid) (γ-PGA) as the backbone of a biodegradable hydrophilic polymer and L-phenylalanine (Phe) as the hydrophobic side chain. γ-PGA is composed of naturally occurring D- and L-glutamic acid, γ-linked together through amide bonds [14–16]. The γ-PGA-*graft*-Phe copolymers can form NPs due to their amphiphilic properties [5]. Their ability to form NPs is attributed to the hydrophobic interactions between the Phe groups attached to

* Corresponding author. Tohoku Graduate University School of Medicine, Department of Ophthalmology, 1-1 Seiryo, Aoba, Sendai, Miyagi 980-8574, Japan. Tel.: +81 22 717 7294; fax: +81 22 717 7298.
E-mail address: ntoru@oph.med.tohoku.ac.jp (T. Nakazawa).

0168-3659/$ – see front matter © 2010 Elsevier B.V. All rights reserved.
doi:10.1016/j.jconrel.2010.11.029

the γ-PGA backbone resulting in the increased stability of the hydrophobic cores in the NPs. NPs consisting of γ-PGA-*graft*-Phe (γ-PGA-Phe NPs) have several important advantages as cytoplasmic delivery carriers including resistance to proteases, such as cathepsin [14], which accumulate in dendritic cells (DCs) and phagocytic cells such as macrophages. Our group [17–20] and others [21] have previously demonstrated that these antigen-loaded NPs represent a possible vaccine candidate for immune therapy. Moreover, γ-PGA-Phe NPs have been tested in several clinical applications including T cell tolerance of pollen antigen [21], vaccination for Japanese encephalitis [17], cancer treatment [18], and human immunodeficiency virus type 1 gp120 [19,20]. Hence, γ-PGA-Phe NPs have the potential for multiple clinical applications in the near future. However, the dynamics of NPs in the eye remains unclear.

In various pathological conditions, monocytes are recruited to the retina through the increased expression of cytokines and chemokines in a damaged area; in addition, resident microglia are also activated, then proliferate and migrate [22,23]. Physiologically, one of the major roles of phagocytic cells is to clean up the debris of dying cells [24]. In various pathological conditions, we have found that macrophages/microglia have a neurodestructive effect on damaged neurons via secreting cytokines or initiating oxidative stress [22,25–27]. Thus, the suppression of macrophages/microglia could be an important strategy for providing neuroprotection in various retinal disorders. In this study, we used γ-PGA-Phe NPs containing Texas Red-labeled ovalbumin (TR-OVA) to explore the dynamics of NPs in the eye. Next, we characterized the effects of γ-PGA-Phe NPs in cultured macrophages and microglia and then investigated the potential for using γ-PGA-Phe NPs containing dexamethasone (DEX-NPs) for *in vivo* immunosuppressive treatment of macrophages and microglia in various pathological conditions in the retinal.

2. Materials and methods

2.1. Animals

In total, 129 Sprague–Dawley (SD) rats (120 male and 9 female, weighing 250–300 g; Japan SLC, Hamamatsu, Japan) were used. For *in vivo* studies, we used 18 male rats (6 for each dosage of the NPs) to study normal conditions, 24 male rats to study the dynamics of NPs under pathological conditions (excitotoxicity and retinal detachment), 16 male rats to study DEX-NP treatment in a retinal detachment model, and 32 male rats to count surviving RGCs after DEX-NP treatment in the excitotoxic model. For *in vitro* experiments, 21 male rats were used for a macrophage culture and 90 rat pups (postnatal day 1 delivered from 9 female SD rats) for primary culture of microglia; another 9 male rats were used for a retina mixed culture. The surgical procedures were performed under deep anesthesia with intramuscular administration of a mixture of ketamine (100 mg/kg) and xylazine (9 mg/kg) or intraperitoneal injections of sodium pentobarbital (45 mg/kg, Vortech Pharmaceuticals). The rats were euthanatized with an intraperitoneal injection of a lethal dose of pentobarbital (Fatal-Plus solution; 390 mg/ml).

All animals were maintained and handled in accordance with the ARVO Statement for the use of animals in Ophthalmic and Vision Research and the guidelines from the declaration of Helsinki and the Guiding Principles in the Care and Use of Animals. All experimental procedures described in the present study were approved by the Ethics Committee for Animal Experiments at Tohoku University Graduate School of Medicine. Animals were treated according to the National Institutes of Health guidelines for the care and use of laboratory animals.

2.2. Materials

γ-PGA ($M_w = 3.8 \times 10^5$, D-Glu/L-Glu = 60/40) was kindly donated by the Meiji Seika Co., Ltd. (Tokyo, Japan). L-phenylalanine ethyl ester (Phe) and dexamethasone (DEX) were purchased from Sigma (St. Louis, MO). 1-Ethyl-3-(3-dimethylaminopropyl) carbodiimide, dimethylsulfoxide (DMSO) and sodium hydrogen carbonate ($NaHCO_3$) were purchased from Wako Pure Chemical Industries (Osaka, Japan). 5-(Aminoacetamido) fluorescein and Texas Red-labeled OVA (TR-OVA) were purchased from Molecular Probes (Eugene, OR).

2.3. Preparation of γ-PGA-Phe NPs

γ-PGA-*graft*-L-phenylalanine (γ-PGA-Phe) was prepared by the conjugation of the L-phenylalanine ethyl ester (Phe) as previously described [14,15]. Briefly, γ-PGA (4.7 unit mmol) was hydrophobically modified by Phe (4.7 mmol) in the presence of 1-Ethyl-3- (3-dimethylaminopropyl) carbodiimide (4.7 mmol) in 50 mM $NaHCO_3$ (100 ml). The purified γ-PGA-Phe was characterized by ^{1}H NMR to determine the degree of Phe grafting. In this study, γ-PGA-Phe with 53% of Phe grafting was used. To analyze the intracellular distribution of the NPs, fluorescein-labeled γ-PGA-Phe (F-γ-PGA-Phe) was also synthesized using the same method in the presence of 5-(aminoacetamido) fluorescein (23.5 μmol). The amount of incorporated fluorescein was measured by spectrofluorometry. NPs composed of γ-PGA-Phe were prepared by a precipitation method. γ-PGA-Phe or F-γ-PGA-Phe (10 mg/ml) was dissolved in DMSO and this solution was added to saline at the same volume to yield a translucent solution. The resulting solution was then centrifuged at 14,000 × *g* for 15 min, rinsed repeatedly, and resuspended in phosphate-buffered saline (PBS) at a concentration of 20 mg/ml.

2.4. Preparation of TR-OVA-encapsulated NPs (TR-OVA-NPs)

To prepare the TR-OVA-encapsulated NPs, γ-PGA-Phe (10 mg/ml in DMSO) was added to the same volume of 2 mg/ml TR-OVA to yield a translucent solution. The resulting solution was centrifuged at 14,000 × *g* for 15 min and repeatedly rinsed to remove the organic solvent and free TR-OVA. Approximately 90% of the initial γ-PGA-Phe copolymer was recovered as NPs. The residual DMSO in the NP solution (20 mg/ml) was removed to below 1 ppm by the purification process. TR-OVA-encapsulated NPs (TR-OVA-NPs) were added to a volume of 4% sodium dodecyl sulfate (SDS) to dissolve the NPs, and the TR-OVA concentration in the TR-OVA-NP solution was measured by the Lowry method, as previously described [28,29]. From the estimated TR-OVA and NP concentrations in the sample solution, TR-OVA-NPs with a TR-OVA loading of 100 μg per milligram NP was prepared. The entrapment efficiency of TR-OVA into the NPs was calculated using the following formula: (amount of encapsulated TR-OVA / initial feeding amount of TR-OVA) × 100. The TR-OVA entrapment efficiency reached approximately 50%.

2.5. Preparation of dexamethasone-adsorbed NPs (DEX-NPs)

To prepare the DEX-NPs, γ-PGA-Phe NPs or F-γ-PGA-Phe NPs (F-NPs) (5 mg/ml in PBS) were mixed with DEX (1 mg/ml in 20% DMSO) at the same volume and the mixture was incubated at 4 °C for 24 h. After the reaction, the NPs or F-NPs were isolated by centrifugation, washed with PBS, and resuspended at 20 mg/ml in PBS. The amount of DEX adsorbed into the NPs was evaluated by a DEX ELISA kit (Neogen, Lexington, KY). The loading content and entrapment efficiency of DEX into the NPs were evaluated in the same manner as was used for the TR-OVA-NPs. DEX-NPs or DEX-F-NPs loaded at 50 μg per milligram NPs were prepared. The entrapment efficiency of DEX into the NPs was calculated using the following formula: (amount of adsorbed DEX / initial feeding amount of DEX) × 100. The DEX entrapment efficiency was approximately 25%.

2.6. Characterization of the NPs

The size of the γ-PGA-Phe NPs in the aqueous solution was measured by a dynamic light scattering (DLS) method using a

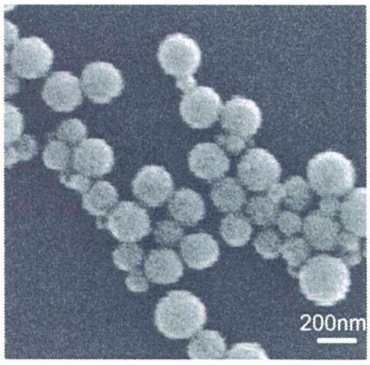

Fig. 1. SEM image of γ-PGA-Phe nanoparticles (NPs). Scale bar = 200 nm.

Zetasizer Nano ZS (Malvern Instruments, UK). The surface charge of the NPs was determined by zeta potential measurements using a Zetasizer Nano ZS. The NP suspension, diluted with PBS (100 μg/ml), was used without filtering to measure both particle size and zeta potential. The mean diameters of NPs, TR-OVA-NPs and DEX-NPs were 175 ± 33, 220 ± 65 and 180 ± 45 nm (mean ± SD), respectively. The zeta potential of the NPs was approximately −25 mV.

(Further information regarding the materials and methods used in this study is contained in "Supplementary data.")

3. Results

3.1. γ-PGA-Phe NPs are taken up by macrophages and microglia in vitro

Macrophages and microglia have been demonstrated to be involved in several pathological conditions of the retina including excitotoxicity [26], retinal detachment [22], and glaucoma [25]. Thus, we first investigated whether NPs can be taken up by those phagocytic cells *in vitro*. In cell culture, 200 nm NPs (Fig. 1) containing TR-OVA were incubated for 2 h and NPs taken up by macrophages and microglia were examined after washing out free TR-OVA-NPs. The signal for TR-OVA (Fig. 2) was co-localized with the cellular markers for macrophages (CD11b) and microglia (CD68) under a fluorescent microscope with 98% of cultured macrophages or microglia containing TR-OVA-NPs (Fig. 2). Analysis using confocal microscopy showed that the TR-OVA-NP signal was detected in the cytoplasm as a high-intensity, granular signal and in macrophages and microglia as a low-intensity, diffuse signal (Fig. 3).

According to flow cytometry analysis (Fig. 4), the TR-OVA-NPs are taken up by macrophages/microglia in a dose-dependent manner, according to the FL2-H histogram. The mean FL2-H indicates that macrophages have a higher capacity for phagocytosis than microglial cells.

3.2. Persistence of NPs in vitro

In our previous study, γ-PGA-Phe NPs were found to be degraded by various enzymes, such as Pronase E and cathepsin B, with different

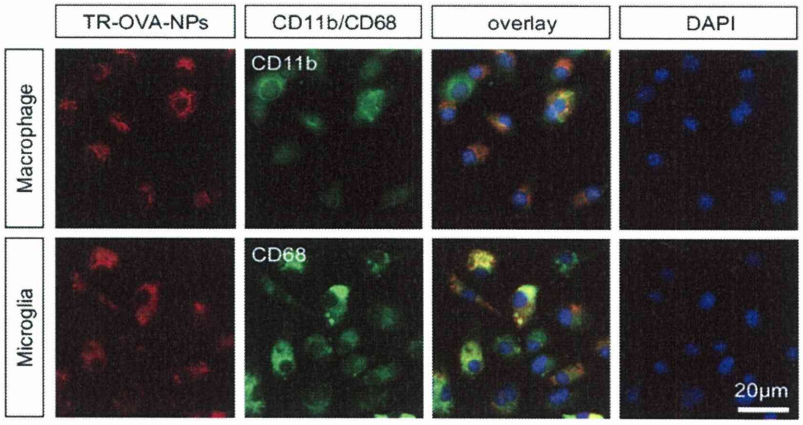

Fig. 2. Uptake of TR-OVA-NPs by cultured macrophages and microglia. The first lines indicate the signals from TR-OVA-NPs and the second lines indicate the immunoreactivity with CD11b, the cellular marker for macrophages (upper panel), and CD68, the marker for activated microglia (lower panel), in the cultured macrophages or microglia. Scale bar = 20 μm.

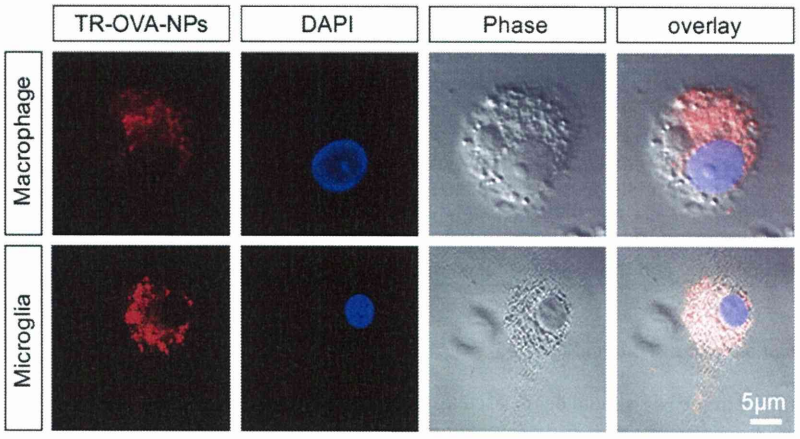

Fig. 3. Confocal images of the cultured macrophages and microglia with TR-OVA-NPs. TR-OVA-NP signaling was detected in the cytoplasm as a high-intensity granular signal and a low-intensity diffuse signal in the cultured macrophages and microglia. Scale bar = 5 μm.

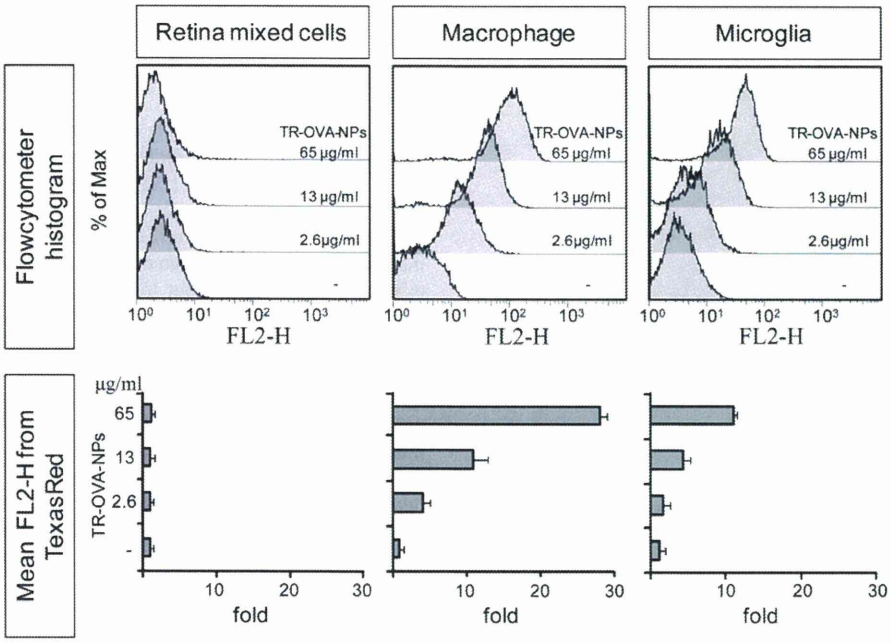

Fig. 4. Relative quantification of phagocytosed TR-OVA-NPs in retinal mixed cells, macrophages, and microglial cells. The histograms demonstrate that the TR-OVA-NPs are taken up by macrophages or microglial cells in a dose-dependent manner and that macrophages have a higher capacity to take up the NPs. TR-OVA-NP (13 μg/ml)-treated macrophages showed an approximately 12-fold increase in the mean FL2-H value compared to the control (0 μg/ml TR-OVA-NPs).

degradation patterns *in vitro*. The degradation and collapse of the NPs was attributed mainly to the cleavage of amide bonds between the α-carboxylate side chains of γ-PGA and Phe [14]. The degradation speed depends on the hydrophobicity (the grafting rate of the hydrophobic side chain) and the type of enzyme, suggesting that there are differences in degradation speeds between cell types. To investigate the degradation speeds and the persistence of TR-OVA-NPs in the cells of interest, the TR-OVA signals were quantified in macrophages and microglia at 2 and 7 days after the administration of NPs. Although the granular signal decreased to 20% on day 7, the diffuse signal remained around 80% in the cytosol of the cell (Fig. 5). According to this result, we presume that TR-OVA-NPs aggregated in cells should release a "granular signal" and the TR-OVA released from degraded NPs that remained in the cytosol should release a "diffuse signal" through the Cy3 filter in the fluorescein microscope. These data may suggest that 80% of the NPs in the macrophages/microglia get degraded on day 7 but that the contents released from the NPs persist in the cytosol.

3.3. NPs in normal and pathological conditions of the retina

To investigate drug dynamics *in vivo*, we injected TR-OVA-NPs into the vitreous cavity, harvested the eyes 2 days later, and prepared cryosections to investigate the distribution of NPs. When 0.8 or 4 μg of NPs were injected into normal, injury-free eyes, no NPs were taken up by the cells (Fig. 6). In the NMDA-damaged retina, resident microglia transformed from a dendritic shape to a spindle or amoeboid shape, reflecting the activated status of the microglia. NPs were taken up by these cells (Fig. 7). In the retinal detachment model, macrophages were recruited into the sub-retinal space and the NPs were taken up (Fig. 8).

3.4. DEX-NPs suppress inflammation both in vitro and in vivo

To be effective, drugs contained in the NPs should be released into the cytoplasm [14].

Thus, an agonist for nuclear receptors or an inhibitor of a signal transduction pathway would be a good target for treatment. Here, we chose DEX as a popular and potent corticosteroid for anti-inflammatory conditions that is already used in the clinic. To test the potential of DEX-NPs to suppress inflammation, we examined changes in the expression of TNFα and MCP-1, major cytokines and chemokines

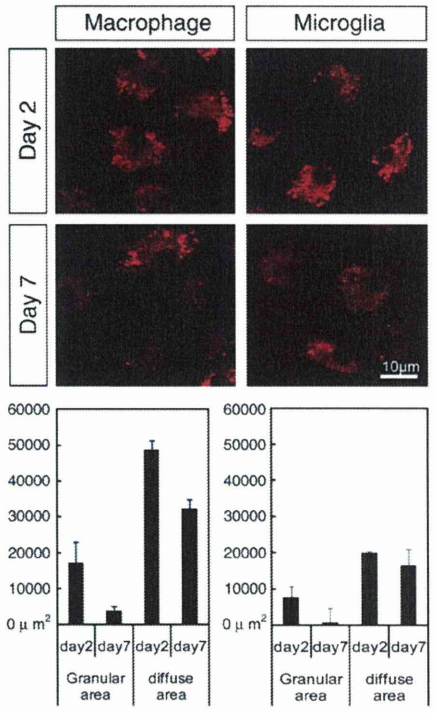

Fig. 5. Time course for the alterations in the persistence of TR-OVA-NPs. The photographs show the appearance of TR-OVA-NPs on day 2 (upper panels) and day 7 (lower panels) *in vitro*. The bar charts show the quantitative data for the area of granular, high-intensity, dot or diffuse cytoplasmic signaling in the cultured macrophages and microglia. Scale bar = 10 μm.

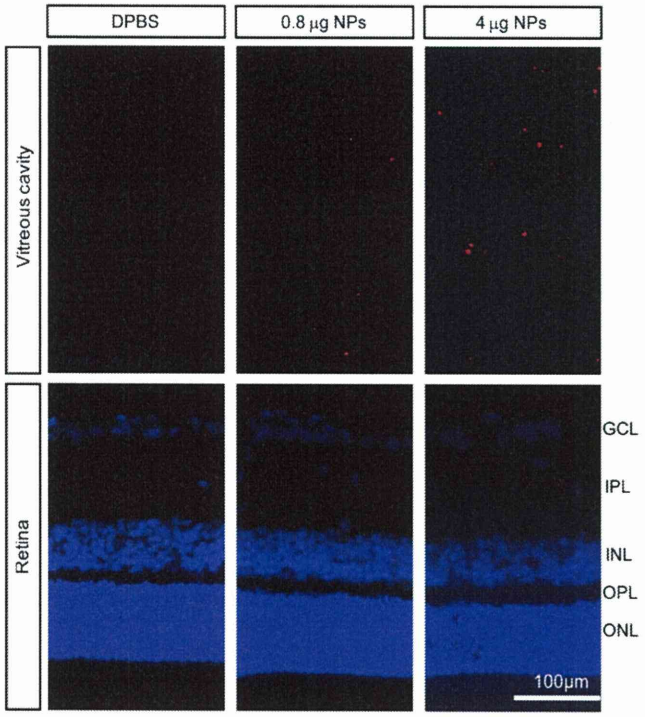

Fig. 6. Absence of accumulation of TR-OVA-NPs in the healthy retina. There was no accumulation of TR-OVA-NPs in the retina (lower panels). Some weak signals were detected in the vitreous cavity but not in any cells. Scale bar = 100 μm. GCL: ganglion cell layer, IPL: inner plexiform layer, INL: inner nuclear layer, OPL: outer plexiform layer, and ONL: outer nuclear layer.

released from cultured macrophages, with or without DEX-NPs (NPs 13 μg/ml, DEX 0.65 μg/ml). As a positive control, we used 0.65 and 6.5 μg/ml of DEX. At 3 and 24 h after application of the NPs, the expression of TNFα and MCP-1 was significantly decreased, with DEX-NPs and pure DEX having almost the same effect (Fig. 9). To investigate whether the released DEX still possessed an anti-inflammatory effect on cultured macrophages, we applied DEX (0.65 μg/ml) or DEX-NPs (13 μg/ml DEX-NPs, equivalent to DEX 0.65 μg/ml) for 2 h and then changed the culture medium to remove the extra compound. We then immediately stimulated the cells with TNFα (day 0) or further culture-treated the macrophages for 48 h (day 2) and then stimulated them with TNFα. After 3 h of TNFα stimulation, the TNFα mRNA was significantly increased both on days 0 and 2. Pretreatment with DEX alone significantly suppressed the TNFα-induced TNFα expression on day 0, but this effect disappeared 2 days after DEX treatment. In contrast, the accumulation of DEX-NPs in macrophages suppressed the TNFα-induced TNFα expression on both days 0 and 2 (Fig. 10). These data suggest that the anti-inflammatory effects of DEX-NPs last longer than that of DEX alone in cultured macrophages. According to our analysis of the degradation of NPs in macrophages (Fig. 5), we believe that the DEX-NPs in macrophages degraded from day 0 to day 7 and kept releasing DEX to suppress the expression of TNFα, although the amount of DEX-NPs in the macrophages and the amount of DEX released into the cytosol of the macrophages was not clear. We next investigated the effects of DEX-NPs when injected intravitreally in rat models of retinal diseases. In the model of NMDA-induced damage, the activation of microglia (ratio of amoeboid shape to resting shape, Fig. 11A) was significantly suppressed by treatment with DEX-NPs (Fig. 11B). At the same time, the DEX-NPs significantly reduced the loss of RGCs 7 days after NMDA treatment (Fig. 12)|.|In the RD model, DEX-NPs significantly decreased the number of TUNEL (+) photoreceptors in the outer nuclear layer 3 days after injury compared with NPs alone (Fig. 13).

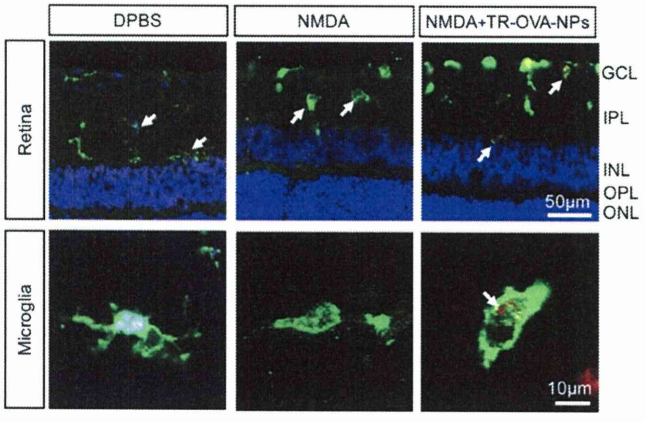

Fig. 7. Accumulation of TR-OVA-NPs in the active microglia in a model of NMDA-induced excitotoxicity. Without treatment with NMDA, microglia had dendrites that were observed to be in the resting phase (left-sided images). Treatment with NMDA induced the activation of microglia (amoeboid shape) in the IPL (center images). The activated microglia phagocytosed the TR-OVA-NPs in the damaged retina (right-sided images). Arrows indicate the microglia in the IPL. Scale bar = 50 μm (upper panels) and 10 μm (lower panels). GCL: ganglion cell layer, IPL: inner plexiform layer, INL: inner nuclear layer, OPL: outer plexiform layer, and ONL: outer nuclear layer.

4. Discussion

In this study, we first investigated the dynamics of γ-PGA-Phe NPs both *in vitro* and *in vivo*. In primary cultures of macrophages and microglia, TR-OVA-NPs were taken up by nearly all macrophages and microglia within which NPs were observed as bright puncta within the cytoplasm. These punctate signals gradually transformed into diffuse signals within the cytoplasm. On day 7, the cytoplasmic levels of TR-OVA were still visible in approximately 60 to 80% of the cells that showed staining on day 2. *In vivo*, the normal, undamaged retina showed no accumulation of NPs. Conversely, intravitreally administered TR-OVA-NPs accumulated in CD11b-positive, recruited macrophages and activated resident microglia in various pathological conditions including NMDA-induced retinal excitotoxicity and retinal detachment. Then, using DEX-NPs, we investigated whether a drug delivered by NPs worked effectively in the damage retina. DEX-NPs significantly suppressed the expression of TNFα and MCP-1 in cultured macrophages following TNFα stimulation. *In vivo*, intravitreal injections of DEX-NPs had a significant neuroprotective effect against NMDA-induced RGCs and RD-induced photoreceptor degeneration. These data suggest that γ-PGA-Phe NPs are a useful tool for the regulation of inflammatory phagocytic cells in the retina, especially under pathological conditions.

γ-PGA-Phe NPs persisted for more than 7 days in cultured macrophages. It has previously been reported that NPs become fragmented in dendritic cells and macrophages [14,28,30]. One purpose of using NPs as a delivery system was to provide more sustained drug release than that achieved when the drug is administered alone. We found that the TR-OVA-NPs were strongly detected at day 2 and that most signals were still present at day 7 in both the macrophages and microglia. Our results using cultured macrophages showed that DEX-NPs, but not soluble DEX alone, continued to suppress TNFα-induced upregulation of TNFα expression 2 days after a 2-h incubation with DEX-NPs followed by the removal of excess NPs from cultured macrophages. We previously demonstrated that macrophages and microglia were major players in the neurodestructive effects of RGCs and photoreceptors in various pathological conditions [22,25]. These data suggest that γ-PGA-NPs

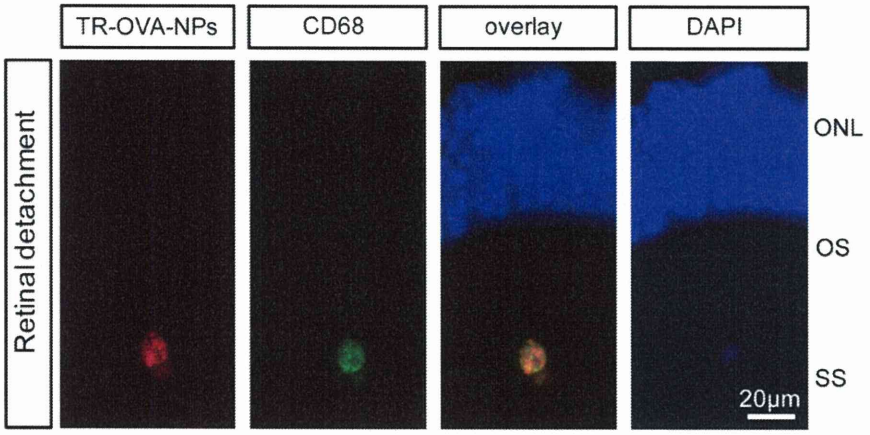

Fig. 8. Accumulation of NPs in the inflamed cells after retinal detachment. In the eye with retinal detachment, TR-OVA-NPs were detected in the recruited monocytes under the sub-retinal space (upper panels) and detected in the recruited CD11b (+) cells in the vitreous cavity. Scale bar = 20 μm. GCL: ganglion cell layer, IPL: inner plexiform layer, ONL: outer nuclear layer, OS: outer segment, and SS: sub-retinal space.

are a potential vehicle for long-term drug delivery in the damaged retina.

The size of the NPs used in this study was approximately 200 nm. This size limits the internalization of NPs to phagocytic cells, as they are too large to diffuse through intact cell membranes. The process of macrophage phagocytosis leads to fragmentation of γ-PGA-Phe by various enzymes (pronase E, protease, cathepsin B, and lipase). In this way, the contents of the NPs are released into the cytosol of the

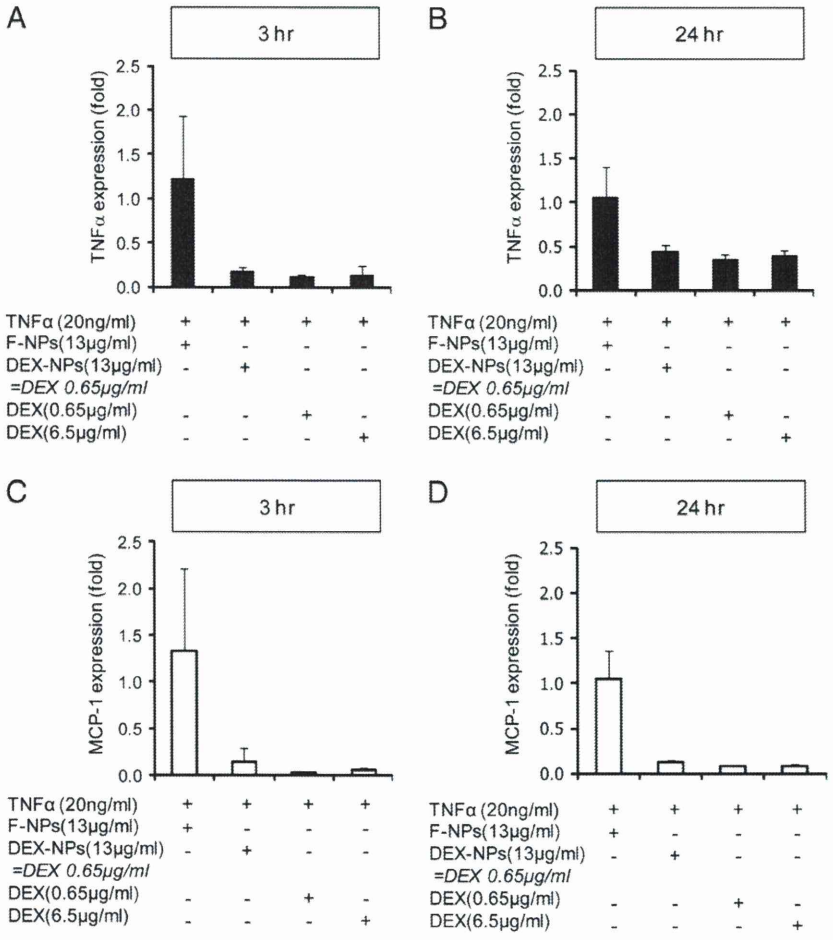

Fig. 9. DEX-NPs suppress the expression of mRNA for TNFα and MCP-1 in the cultured macrophages. The bar charts demonstrate the expressional changes of TNFα and MCP-1 at 3 h (upper panels) and 24 h (lower panels) *in vitro*. Both DEX-NPs and DEX alone had a similar potential for suppressing the activated macrophages.

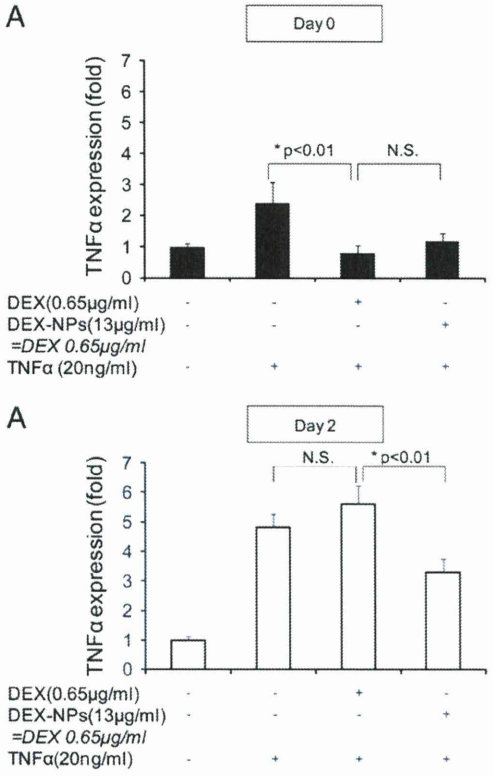

Fig. 10. DEX-NPs had a longer anti-inflammatory effect in the cultured macrophages. The bar charts show the expressional changes of TNFα at 2 h after TNFα stimulation. After 2 h of incubation, DEX-NPs and DEX alone had a similar potential for suppressing TNFα-induced macrophage activation.

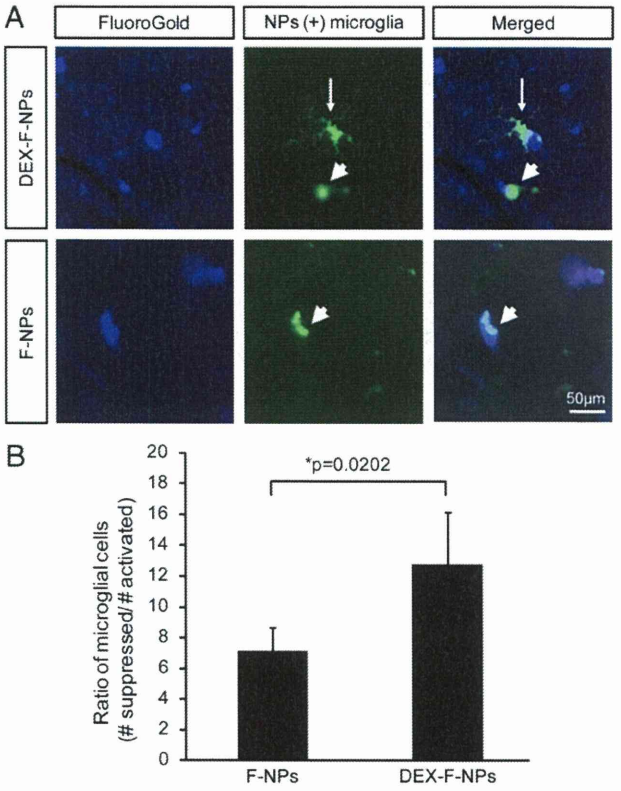

Fig. 11. The effect of DEX-NPs on NMDA-induced microglial activation. A: A representative photograph of the flat-mounted retina 7 days after injury with NMDA. DEX-F-NPs (A: upper panels), but not F-NPs (A: lower panels), suppress the morphological changes in microglia from NMDA-induced retinal damage. The white arrow indicates the resting microglia (ramified shapes) and the arrowheads indicate the activated microglia (amoeboid shapes). B: Quantitative data for the ratio of the numbers of "suppressed microglia" and "activated microglia". Scale bar = 50 μm.

phagocytic cells. Hence, various other molecules are potential candidates to be used with this delivery platform, including ligands for nuclear receptors or modulators of signal transduction, transcription, or translation. In this study, in order to investigate whether released drugs were effective, we chose DEX because it binds to a nuclear receptor. Other possible uses of γ-PGA-Phe NPs could be to deliver small peptides, siRNA, antisense DNA, and various small compounds. The use of PLA and PLGA, other common candidates for drug delivery systems, is limited by the choice of molecules. Thus, γ-PGA-Phe NPs enabled us to specifically target macrophages and microglia using various approaches.

Clinically, steroids are potent drugs to suppress inflammation. Subtenon or intravitreal administration of triamcinolone acetate (IVTA), a type of steroid, has been effective in the treatment of several retinal disorders, including uveitis, diabetic macular edema, laser injury, and branch or central retinal vein occlusion [31,32]. However, 30 to 40% of patients with IVTA experienced complications of steroid-induced glaucoma [33–35] and post-capsular cataract formation [36], and 59% of patients with preexisting glaucoma required additional glaucoma medications [33]. Furthermore, direct administration of steroids is toxic for retinal neurons [37]. Our results suggest that γ-PGA-Phe NPs open a new avenue for minimizing the complications of steroid treatment by specifically targeting macrophages and microglia. These NPs have been applied to several systemic diseases including T cell tolerance for pollen antigen [21] and vaccination for Japanese encephalitis [17], cancer [18], and human immunodeficiency virus type 1 gp120 [19,20]. Thus, further studies on the safety and efficacy of γ-PGA-Phe NPs as a potent candidate for drug delivery in retinal disorders seem warranted.

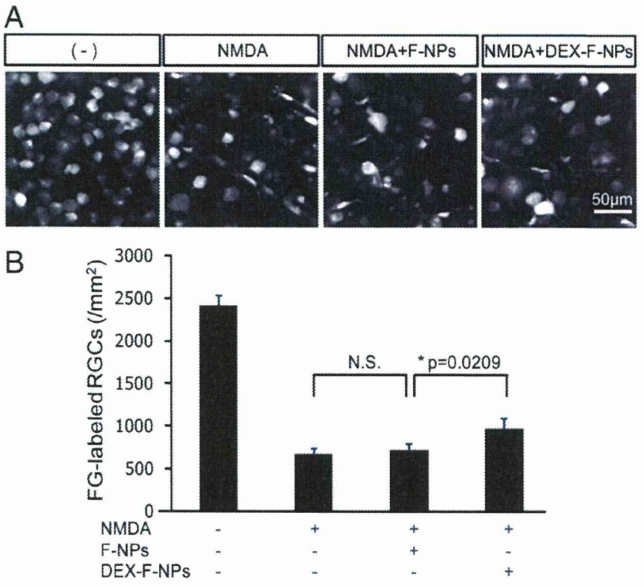

Fig. 12. DEX-F-NPs suppressed NMDA-induced RGC death. A: A representative photograph of FG-labeled RGCs in the flat-mounted retina 7 days after NMDA injection. B: Quantitative data for FG-labeled RGCs. DEX-F-NPs, but not F-NPs, suppressed NMDA-induced RGC death.

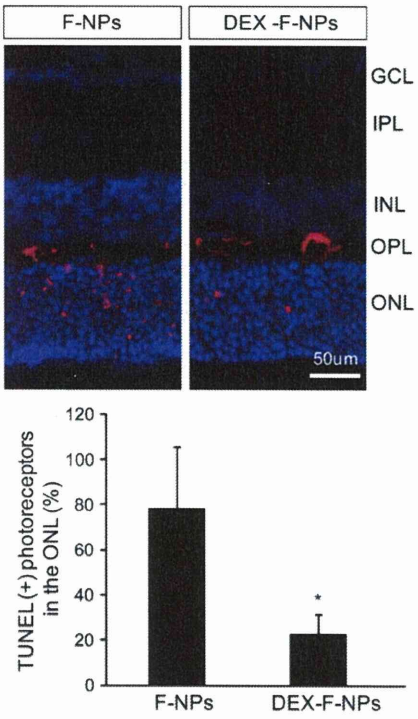

Fig. 13. DEX-NPs suppress retinal detachment-induced photoreceptor degeneration. The upper panels show the TUNEL (+) cells (red signals) and DAPI-nuclear staining (blue signals). The bar charts in the lower panels show the quantitative data from TUNEL (+) photoreceptors in the ONL and suggest that the DEX-NPs significantly suppressed the number of TUNEL (+) cells (*: $p = 0.0065$). Scale bar = 50 μm. GCL: ganglion cell layer, IPL: inner plexiform layer, INL: inner nuclear layer, OPL: outer plexiform layer, and ONL: outer nuclear layer.

Acknowledgements

We thank Prof. Larry. I. Benowitz (Children's Hospital, Harvard Medical School) for editing this manuscript and Mr. Jiro Watanabe and Koutaro Yamamoto for technical assistance. This study was supported by Grants-in-Aid from the Ministry of Education, Science and Technology of Japan (21659395 and 22689045, T.N.), the Uehara Memorial Research Foundation, the Takeda Research Foundation, the Imai Glaucoma Research Foundation (T.N.), and CREST from the Japan Science and Technology Agency (T. A. and M. A.).

Appendix A. Supplementary data

Supplementary data to this article can be found online at doi:10.1016/j.jconrel.2010.11.029.

References

[1] D. Ghate, H.F. Edelhauser, Ocular drug delivery, Expert Opin. Drug Deliv. 3 (2) (2006) 275–287.
[2] R. Gurny, T. Boye, H. Ibrahim, Ocular therapy with nanoparticulate systems for controlled drug delivery, J. Control. Release 2 (1985) 353–361.
[3] J.A. Champion, Y.K. Katare, S. Mitragotri, Particle shape: a new design parameter for micro- and nanoscale drug delivery carriers, J. Control. Release 121 (1–2) (2007) 3–9.
[4] U.B. Kompella, N. Bandi, S.P. Ayalasomayajula, Subconjunctival nano- and microparticles sustain retinal delivery of budesonide, a corticosteroid capable of inhibiting VEGF expression, Investig. Ophthalmol. Vis. Sci. 44 (3) (2003) 1192–1201.
[5] H. Kranz, N. Ubrich, P. Maincent, R. Bodmeier, Physicomechanical properties of biodegradable poly(D, L-lactide) and poly(D, L-lactide-co-glycolide) films in the dry and wet states, J. Pharm. Sci. 89 (12) (2000) 1558–1566.
[6] C.X. Song, V. Labhasetwar, H. Murphy, X. Qu, W.R. Humphrey, R.J. Shebuski, R.J. Levy, Formulation and characterization of biodegradable nanoparticles for intravascular local drug delivery, J. Control. Release 43 (2–3) (1997) 197–212.
[7] H.M. Redhead, S.S. Davis, L. Illum, Drug delivery in poly (lactide-co-glycolide) nanoparticles surface modified with poloxamer 407 and poloxamine 908: in vitro characterisation and in vivo evaluation, J. Control. Release 70 (3) (2001) 353–363.
[8] J.H. Kim, K.W. Kim, M.H. Kim, Y.S. Yu, Intravenously administered gold nanoparticles pass through the blood-retinal barrier depending on the particle size, and induce no retinal toxicity, Nanotechnology 20 (50) (2009) 505101.
[9] K. Okabe, H. Kimura, J. Okabe, A. Kato, N. Kunou, Y. Ogura, Intraocular tissue distribution of betamethasone after intrascleral administration using a non-biodegradable sustained drug delivery device, Investig. Ophthalmol. Vis. Sci. 44 (6) (2003) 2702–2707.
[10] N. Kunou, Y. Ogura, M. Hashizoe, Y. Honda, S.H. Hyon, Y. Ikada, Controlled intraocular delivery of ganciclovir with use of biodegradable scleral implant in rabbits, J. Control. Release 37 (1–2) (1995) 143–150.
[11] E. Eljarrat-Binstock, A.J. Domb, Iontophoresis: a non-invasive ocular drug delivery, J. Control. Release 110 (3) (2006) 479–489.
[12] E. Eljarrat-Binstock, F. Raiskup, J. Frucht-Pery, A.J. Domb, Transcorneal and transscleral iontophoresis of dexamethasone phosphate using drug loaded hydrogel, J. Control. Release 106 (3) (2005) 386–390.
[13] G. Zhang, X. Feng, K. Wabner, C. Fandrey, A. Naqwi, T. Wiedmann, T.W. Olsen, Intraocular nanoparticle drug delivery: a pilot study using an aerosol during pars plana vitrectomy, Investig. Ophthalmol. Vis. Sci. 48 (11) (2007) 5243–5249.
[14] T. Akagi, M. Higashi, T. Kaneko, T. Kida, M. Akashi, Hydrolytic and enzymatic degradation of nanoparticles based on amphiphilic poly(gamma-glutamic acid)-graft-L-phenylalanine copolymers, Biomacromolecules 7 (1) (2006) 297–303.
[15] T. Akagi, X. Wang, T. Uto, M. Baba, M. Akashi, Protein direct delivery to dendritic cells using nanoparticles based on amphiphilic poly(amino acid) derivatives, Biomaterials 28 (23) (2007) 3427–3436.
[16] I.L. Shih, Y.T. Van, The production of poly-(gamma-glutamic acid) from microorganisms and its various applications, Bioresour. Technol. 79 (3) (2001) 207–225.
[17] S. Okamoto, H. Yoshii, T. Ishikawa, T. Akagi, M. Akashi, M. Takahashi, K. Yamanishi, Y. Mori, Single dose of inactivated Japanese encephalitis vaccine with poly (gamma-glutamic acid) nanoparticles provides effective protection from Japanese encephalitis virus, Vaccine 26 (5) (2008) 589–594.
[18] T. Yoshikawa, N. Okada, A. Oda, K. Matsuo, H. Kayamuro, Y. Ishii, T. Yoshinaga, T. Akagi, M. Akashi, S. Nakagawa, Nanoparticles built by self-assembly of amphiphilic gamma-PGA can deliver antigens to antigen-presenting cells with high efficiency: a new tumor-vaccine carrier for eliciting effector T cells, Vaccine 26 (10) (2008) 1303–1313.
[19] X. Wang, T. Uto, T. Akagi, M. Akashi, M. Baba, Induction of potent CD8+ T-cell responses by novel biodegradable nanoparticles carrying human immunodeficiency virus type 1 gp120, J. Virol. 81 (18) (2007) 10009–10016.
[20] X. Wang, T. Uto, T. Akagi, M. Akashi, M. Baba, Poly(gamma-glutamic acid) nanoparticles as an efficient antigen delivery and adjuvant system: potential for an AIDS vaccine, J. Med. Virol. 80 (1) (2008) 11–19.
[21] T. Yoshitomi, K. Hirahara, J. Kawaguchi, N. Serizawa, Y. Taniguchi, S. Saito, M. Sakaguchi, S. Inouye, A. Shiraishi, Three T-cell determinants of Cry j 1 and Cry j 2, the major Japanese cedar pollen antigens, retain their immunogenicity and tolerogenicity in a linked peptide, Immunology 107 (4) (2002) 517–522.
[22] T. Nakazawa, T. Hisatomi, C. Nakazawa, K. Noda, K. Maruyama, H. She, A. Matsubara, S. Miyahara, S. Nakao, Y. Yin, L. Benowitz, A. Hafezi-Moghadam, J.W. Miller, Monocyte chemoattractant protein 1 mediates retinal detachment-induced photoreceptor apoptosis, Proc. Natl Acad. Sci. USA 104 (7) (2007) 2425–2430.
[23] T. Nakazawa, A. Matsubara, K. Noda, T. Hisatomi, H. She, D. Skondra, S. Miyahara, L. Sobrin, K.L. Thomas, D.F. Chen, C.L. Grosskreutz, A. Hafezi-Moghadam, J.W. Miller, Characterization of cytokine responses to retinal detachment in rats, Mol. Vis. 12 (2006) 867–878.
[24] T. Hisatomi, T. Sakamoto, K.H. Sonoda, C. Tsutsumi, H. Qiao, H. Enaida, I. Yamanaka, T. Kubota, T. Ishibashi, S. Kura, S.A. Susin, G. Kroemer, Clearance of apoptotic photoreceptors: elimination of apoptotic debris into the subretinal space and macrophage-mediated phagocytosis via phosphatidylserine receptor and integrin alphavbeta3, Am. J. Pathol. 162 (6) (2003) 1869–1879.
[25] T. Nakazawa, C. Nakazawa, A. Matsubara, K. Noda, T. Hisatomi, H. She, N. Michaud, A. Hafezi-Moghadam, J.W. Miller, L.I. Benowitz, Tumor necrosis factor-alpha mediates oligodendrocyte death and delayed retinal ganglion cell loss in a mouse model of glaucoma, J. Neurosci. 26 (49) (2006) 12633–12641.
[26] T. Nakazawa, H. Takahashi, K. Nishijima, M. Shimura, N. Fuse, M. Tamai, A. Hafezi-Moghadam, K. Nishida, Pitavastatin prevents NMDA-induced retinal ganglion cell death by suppressing leukocyte recruitment, J. Neurochem. 100 (4) (2007) 1018–1031.
[27] K. Noda, S. Miyahara, T. Nakazawa, L. Almulki, S. Nakao, T. Hisatomi, H. She, K.L. Thomas, R.C. Garland, J.W. Miller, E.S. Gragoudas, Y. Kawai, Y. Mashima, A. Hafezi-Moghadam, Inhibition of vascular adhesion protein-1 suppresses endotoxin-induced uveitis, Faseb J. 22 (4) (2008) 1094–1103.
[28] T. Akagi, T. Kaneko, T. Kida, M. Akashi, Preparation and characterization of biodegradable nanoparticles based on poly(gamma-glutamic acid) with l-phenylalanine as a protein carrier, J. Control. Release 108 (2–3) (2005) 226–236.
[29] T. Akagi, T. Kaneko, T. Kida, M. Akashi, Multifunctional conjugation of proteins on/into bio-nanoparticles prepared by amphiphilic poly(gamma-glutamic acid), J. Biomater. Sci. Polym. Ed. 17 (8) (2006) 875–892.
[30] T. Yoshikawa, N. Okada, A. Oda, K. Matsuo, Y. Mukai, Y. Yoshioka, T. Akagi, M. Akashi, S. Nakagawa, Development of amphiphilic gamma-PGA-nanoparticle based tumor vaccine: potential of the nanoparticulate cytosolic protein delivery carrier, Biochem. Biophys. Res. Commun. 366 (2) (2008) 408–413.
[31] M. Shimura, T. Nakazawa, K. Yasuda, T. Shiono, T. Iida, T. Sakamoto, K. Nishida, Comparative therapy evaluation of intravitreal bevacizumab and triamcinolone

acetonide on persistent diffuse diabetic macular edema, Am. J. Ophthalmol. 145 (5) (2008) 854–861.
[32] M. Shimura, T. Nakazawa, K. Yasuda, T. Shiono, K. Nishida, Pretreatment of posterior subtenon injection of triamcinolone acetonide has beneficial effects for grid pattern photocoagulation against diffuse diabetic macular oedema, Br. J. Ophthalmol. 91 (4) (2007) 449–454.
[33] J. Baath, A.L. Ells, A. Crichton, A. Kherani, R.G. Williams, Safety profile of intravitreal triamcinolone acetonide, J. Ocul. Pharmacol. Ther. 23 (3) (2007) 304–310.
[34] L.I. Lau, K.C. Chen, F.L. Lee, S.J. Chen, Y.C. Ko, C.J. Liu, W.M. Hsu, Intraocular pressure elevation after intravitreal triamcinolone acetonide injection in a Chinese population, Am. J. Ophthalmol. 146 (4) (2008) 573–578.
[35] M. Shimura, K. Yasuda, T. Nakazawa, T. Shiono, T. Sakamoto, K. Nishida, Drug reflux during posterior subtenon infusion of triamcinolone acetonide in diffuse diabetic macular edema not only brings insufficient reduction but also causes elevation of intraocular pressure, Graefes Arch. Clin. Exp. Ophthalmol. 247 (7) (2009) 907–912.
[36] A. Galor, R. Margolis, O.M. Brasil, V.L. Perez, P.K. Kaiser, J.E. Sears, C.Y. Lowder, S.D. Smith, Adverse events after intravitreal triamcinolone in patients with and without uveitis, Ophthalmology 114 (10) (2007) 1912–1918.
[37] H. Chung, J.J. Hwang, J.Y. Koh, J.G. Kim, Y.H. Yoon, Triamcinolone acetonide-mediated oxidative injury in retinal cell culture: comparison with dexamethasone, Investig. Ophthalmol. Vis. Sci. 48 (12) (2007) 5742–5749.

Clinical Ophthalmology

Dovepress
open access to scientific and medical research

Open Access Full Text Article

ORIGINAL RESEARCH

Preoperative factors predictive of postoperative decimal visual acuity ≥ 1.0 following surgical treatment for idiopathic epiretinal membrane

Hiroshi Kunikata[1]
Toshiaki Abe[2]
Jiro Kinukawa[1]
Kohji Nishida[1,3]

[1]Department of Ophthalmology and Visual Science, Tohoku University Graduate School of Medicine, Sendai, Japan; [2]Division of Clinical Cell Therapy, Tohoku University Graduate School of Medicine, Sendai, Japan; [3]Department of Ophthalmology, Osaka University Medical School, Suita, Japan

Purpose: To report the preoperative best-corrected visual acuity (BCVA) and foveal thickness (FT) values that lead to a postoperative decimal BCVA of ≥1.0 after surgical removal of an idiopathic epiretinal membrane (ERM).

Methods: This is a retrospective case series of 73 eyes that underwent surgery for removal of an idiopathic ERM. All eyes had been treated by a single surgeon using a 25-gauge transconjunctival sutureless vitrectomy and indocyanine green-assisted internal limiting membrane peel. The BCVA and FT were measured at baseline and 6 months postoperatively.

Results: A postoperative decimal BCVA ≥ 1.0 was obtained in eyes with a preoperative decimal BCVA ≥ 0.3 but not in those with a preoperative decimal BCVA ≤ 0.2. The incidence of obtaining a postoperative decimal BCVA ≥ 1.0 was significantly ($P = 0.002$) higher in eyes with a preoperative decimal BCVA ≥ 0.5 (50%) than in eyes with a preoperative decimal BCVA < 0.5 (11%). Additionally, a postoperative decimal BCVA of ≥1.0 was obtained in 51% of the eyes that had a preoperative FT < 400 μm, compared with only 21% of eyes with a preoperative FT ≥ 400 μm ($P = 0.01$). The incidence of obtaining a postoperative decimal BCVA ≥ 1.0 was significantly higher in eyes with preoperative decimal BCVA ≥ 0.5 and FT < 400 μm (60%) than in eyes with preoperative decimal BCVA ≥ 0.5 and FT ≥ 400 μm (20%; $P = 0.03$) or preoperative BCVA < 0.5 and FT ≥ 400 μm (7%; $P < 0.001$).

Conclusions: These findings indicate that eyes with both preoperative BCVA ≥ 0.5 and FT < 400 μm have a significantly better chance of obtaining a postoperative decimal BCVA ≥ 1.0 following idiopathic ERM removal.

Keywords: 25-gauge vitrectomy, optical coherence tomography, epimacular membrane, epiretinal membrane, visual acuity, foveal thickness

Introduction

The surgical indications for the removal of an epiretinal membrane (ERM) have not been standardized. The removal of an ERM is helpful for many patients, but the surgical complications, such as endophthalmitis and retinal detachment, can negate the effectiveness of the removal.[1–3] Because eyes with an idiopathic ERM have moderately good preoperative vision, the eyes to undergo surgery to remove an ERM should be carefully selected. The selection depends on the patient's symptoms and visual requirements, and the vitreous surgeon's technique. A postoperative decimal best-corrected visual acuity (BCVA) ≥ 1.0 (BCVA Snellen chart ≥ 20/20) is a positive result of removing an idiopathic ERM.[4–7]

A 25-gauge transconjunctival sutureless vitrectomy (25G-TSV) and membranectomy for the treatment of idiopathic ERM was first reported in 2002 by Fuji et al.[8,9] This

Correspondence: Hiroshi Kunikata
Department of Ophthalmology and Visual Science, Tohoku University Graduate School of Medicine, 1-1 Seiryo-machi, Aoba-ku, Sendai 980-8574, Japan
Tel +81 22 717 7294
Fax +81 22 717 7298
Email kunikata@oph.med.tohoku.ac.jp

submit your manuscript | www.dovepress.com
Dovepress
DOI: 10.2147/OPTH.S15848

procedure has evolved and become more common over the years. The main advantage of this technique is that the intraoperative procedure is sutureless, meaning that the wounds are self-sealing. This reduces postoperative ocular pain and discomfort and procedure time, as well as the complications (eg, inflammation, astigmatism). In addition, using a 25G-TSV for the treatment of an idiopathic ERM leads to earlier postoperative visual improvement, compared with conventional 20-gauge vitrectomy.[10,11] Because 25G-TSV retains the vitreous, the possibility of endophthalmitis has been discussed for many years, but a recent multicenter report of over 40,000 cases indicated no difference.[12]

Though there are many reports of postoperative favorable visual outcomes and visual improvements that may not be exactly defined as decimal BCVA $\geq$ 1.0, we could not find any reports on preoperative findings that ensure a postoperative decimal BCVA $\geq$ 1.0 in patients with ERMs. The purpose of this study was to determine the preoperative BCVA and foveal thickness (FT) in eyes with an idiopathic ERM that would help predict a postoperative BCVA $\geq$ 1.0 following 25G-TSV/membranectomy.

Patients and methods

Participants

This was a retrospective case series of 73 eyes of 73 patients with idiopathic ERMs who underwent 25G-TSV (Alcon Laboratories; Fort Worth, TX, USA)/membranectomy. The inclusion criterion was a clinically detectable idiopathic ERM diagnosed by fundus examination or optical coherence tomography (OCT), causing a decrease of visual acuity or metamorphopsia as reported by the patient; a questionnaire; or Amsler grid findings. The exclusion criteria included prior vitreous surgery, prior intravitreal injection of triamcinolone acetonide or antivascular endothelial growth factor, ocular inflammation, prior scleral buckling, prior trauma, and eyes with complex vitreoretinal disease such as proliferative vitreoretinopathy or proliferative diabetic retinopathy. None of the patients was excluded because of a decimal BCVA < 0.05. The preoperative demographics of the patients are shown in Table 1.

All of the surgeries were performed at the Surgical Retina Clinic of the Tohoku University Hospital, Sendai, Japan, from July 2006 to November 2008. After the purpose and procedures of the operation were explained, an informed consent was obtained from all patients. The procedures used conformed to the tenets of the Declaration of Helsinki and were approved by the Review Board of the School of Medicine, Tohoku University.

Table 1 Summary of clinical data

Characteristics	Value	*P* value
Eyes (no.)	73	
Patients (no./%)	73	
Male	24 (33)	
Female	49 (67)	
Age (yrs)		
Mean ± SD	67.2 ± 10.4	
Median	68	
Range	28–87	
Lens status (baseline; no./%)		
Phakic	61 (84)	
Pseudophakic	12 (16)	
Surgical procedure (no./%)		
25G-TSV	34 (47)	
Triple surgery	39 (53)	
Decimal BCVA (mean)		
Baseline	0.59	
Postoperative 6M	0.74	
BCVA (logMAR; mean ± SD)		
Baseline	0.23 ± 0.25	
Postoperative 6M	0.13 ± 0.27	<0.001*
Improvement	0.10 ± 0.21	
Foveal thickness (μm; mean (SD)		
Baseline	371 ± 106	
Postoperative 6M	300 ± 67	<0.001*
Reduction	71 ± 43	

Notes: *Wilcoxon signed–rank test, Postoperative 6M versus baseline. Triple surgery, phaceomulsification and aspiration, intraocularlens implant, and 25-gauge transconjunctival sutureless vitrectomy.

Abbreviations: SD, standard deviation; 25G-TSV, 25-gauge transconjunctival sutureless vitrectomy; BCVA, best-corrected visual acuity; logMAR, logarithm of the minimum angle of resolution.

Surgical procedures

All surgeries were performed under retrobulbar anesthesia by a single surgeon (HK). A conjunctival peritomy was not made in all cases, and all surgeries were performed with the 25G Accurus Vitrectomy System (Alcon Laboratories). Patients with concomitant lenticular changes had a combined sutureless 25G-TSV and phacoemulsification.

After resecting the vitreal core, about 4 mg of triamcinolone acetonide (TA; Kenacort-A, Bristol-Myers Squibb, Tokyo, Japan) was injected into the vitreous cavity to determine whether a posterior vitreous detachment (PVD) was present. If a PVD was not present, we created a PVD with a 25-gauge cutter. After creating a PVD and removing residual gel, the epiretinal membrane was removed without using any dye. In addition, the internal limiting membrane (ILM) was removed using indocyanine green (ICG; Santen Co., Osaka, Japan) to improve visibility. The ICG crystals were reconstituted in 1.00 mL distilled water to produce a concentration of 25 mg/mL. Further dilutions were made with

19 mL balanced salt solution. Thus, the final concentration of ICG was 1.25 mg/mL, and approximately 0.2 mL of it was injected around the ERM.

Postoperatively, both antibiotics and corticosteroids were injected subconjunctivally in all cases. We used topical nonsteroidal anti-inflammatory drugs for all cases for at least 3 months after the membrane peel.

Measurements of clinical findings

All of the patients had a complete ophthalmological examination, including BCVA and FT measurements preoperatively and at 6 months postoperatively. The BCVA was determined with a standard Japanese Landolt visual acuity chart. FT was measured by OCT (Zeiss-Humphrey model OCT-3000, Dublin, CA, USA) before and after the 25G-TSV. The retinal thickness of the central fovea was defined as the distance between the ILM and the retinal pigment epithelium and was automatically calculated by the software of the OCT.

Statistical analyses

The data are presented as mean ± standard deviation. The significance of the differences between the pre- and post-25G-TSV data was determined by Wilcoxon signed-rank tests. To obtain a postoperative decimal BCVA ≥ 1.0, the distribution of preoperative decimal BCVA and preoperative FT was assessed by Fisher's exact probability test. The decimal BCVA was converted to a logarithm of the minimal angle resolution (logMAR) units for statistical analyses. Spearman's rank correlation coefficient was calculated to determine the correlation between postoperative BCVA (logMAR) and preoperative BCVA (logMAR), and between postoperative BCVA (logMAR) and preoperative FT. A P value < 0.05 was considered to be statistically significant.

Results

A summary of the clinical data is shown in Table 1. The patients included 24 men and 49 women whose mean ± standard deviation age was 67.2 ± 10.4 years. The mean postoperative follow-up period was 9.8 ± 3.5 months with a range of 6–21 months. The mean preoperative BCVA was 0.59 (decimal) or 0.23 logMAR units. Phacoemulsification and aspiration, intraocular lens implantation, and 25G-TSV were performed on 39 eyes (53%), and 25G-TSV only was performed on 34 eyes (47%). In the 22 phakic eyes that had ERM surgery without cataract surgery, there was only one patient whose lens sclerosis progressed postoperatively, and cataract surgery was performed after 5 months from the initial ERM surgery. None of the patients required suturing of the sclerotomy site at the end of the initial surgery.

The mean postoperative BCVA at 6 months was 0.13 ± 0.27 logMAR units, which was significantly better than the preoperative BCVA of 0.23 ± 0.25 logMAR units ($P < 0.001$, Wilcoxon signed-rank test). The mean postoperative FT was 300 ± 67 μm, which was significantly thinner than the preoperative FT of 371 ± 106 μm ($P < 0.001$, Wilcoxon signed-rank test).

A summary of the correlations between the BCVA and FT is shown in Table 2. The preoperative BCVA (in logMAR units) was significantly correlated to the preoperative FT ($r = 0.43$, $P < 0.001$, Spearman's rank correlation coefficient). The postoperative BCVA was significantly correlated with the postoperative FT ($r = 0.26$, $P = 0.03$, Spearman's rank correlation coefficient). The preoperative BCVA was significantly correlated with the postoperative BCVA ($r = 0.44$, $P < 0.001$, Spearman's rank correlation coefficient, Figure 1). The preoperative FT was also significantly correlated with the postoperative BCVA ($r = 0.24$, $P = 0.04$, Spearman's rank correlation coefficient, Figure 2). The mean of the visual improvement (preoperative BCVA – postoperative BCVA in logMAR units) was 0.10 logMAR units, and this improvement was correlated with the preoperative BCVA ($r = 0.55$, $P < 0.001$, Spearman's rank correlation coefficient). Thus, the postoperative visual improvement was greater in eyes with initially poorer preoperative vision. However, the postoperative visual improvement was not significantly correlated with the preoperative FT ($r = 0.21$, $P = 0.07$, Spearman's rank correlation coefficient). The reduction of FT (preoperative FT – postoperative FT) was strongly correlated with the preoperative FT ($r = 0.80$, $P < 0.001$, Spearman's rank correlation coefficient). The reduction of FT was greater in

Table 2 Correlation between visual acuity and foveal thickness

		r value	P value
Reduction of FT	Preoperative FT	0.80	<0.001*
Visual improvement	Preoperative BCVA	0.55	<0.001*
Postoperative BCVA	Preoperative BCVA	0.44	<0.001*
Preoperative BCVA	Preoperative FT	0.43	<0.001*
Reduction of FT	Preoperative BCVA	0.31	0.008*
Postoperative BCVA	Postoperative FT	0.26	0.03*
Visual improvement	Reduction of FT	0.24	0.04*
Postoperative BCVA	Preoperative FT	0.24	0.04*

Notes: *Spearman's correlation coefficient by rank. Reduction of FT, preoperative FT – postoperative FT; Visual improvement, preoperative BCVA – postoperative BCVA in logMAR units.

Abbreviations: FT, foveal thickness (μm); BCVA, best-corrected visual acuity in logarithm of the minimum angle of resolution (logMAR).

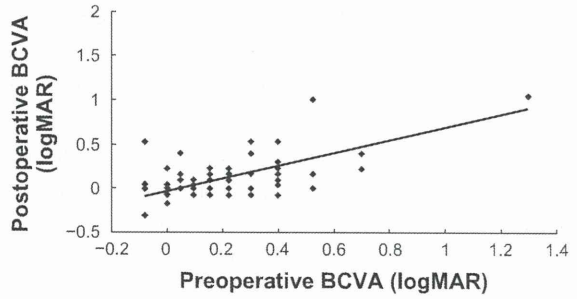

Figure 1 Coefficients of correlation between postoperative and preoperative BCVA. The postoperative BCVA at 6 months is significantly correlated with the preoperative BCVA ($r = 0.44$, $P < 0.001$, Spearman's rank correlation coefficient).
Abbreviations: BCVA, best-corrected visual acuity; logMAR, logarithm of the minimum angle of resolution.

eyes with thicker preoperative FT. The reduction of FT was also significantly correlated with the preoperative BCVA and postoperative visual improvement ($r = 0.31$, $P = 0.008$, and $r = 0.24$, $P = 0.04$, respectively, Spearman's rank correlation coefficient).

The associations between a preoperative decimal BCVA and a postoperative decimal BCVA ≥ 1.0 are shown in Table 3. A postoperative decimal BCVA ≥ 1.0 was obtained in 29 eyes with a preoperative decimal BCVA ≥ 0.3, but none of the eyes with a preoperative decimal BCVA ≤ 0.2 showed a postoperative decimal BCVA ≥ 1.0. The likelihood of obtaining a postoperative decimal BCVA ≥ 1.0 was 57% (12/21 eyes) in eyes with a preoperative decimal BCVA ≥ 0.9, 47% (7/15 eyes) in eyes with preoperative decimal BCVA of 0.7–0.8, 44% (8/18 eyes) in eyes with preoperative decimal BCVA of 0.5–0.6, and 13% (2/15 eyes) in eyes with preoperative decimal BCVA of 0.3–0.4. The likelihood of obtaining a postoperative decimal BCVA ≥ 1.0 was significantly higher in eyes with a preoperative decimal BCVA ≥ 0.9 than preoperative

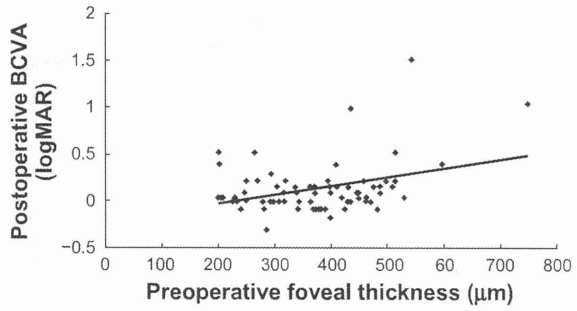

Figure 2 Coefficients of correlation between postoperative BCVA and preoperative foveal thickness. The postoperative BCVA at 6 months was significantly correlated with the preoperative foveal thickness ($r = 0.24$, $P = 0.04$, Spearman's rank correlation coefficient).
Abbreviations: BCVA, best-corrected visual acuity; logMAR, logarithm of the minimum angle of resolution.

Table 3 Association between preoperative decimal best-corrected visual acuity and postoperative decimal best-corrected visual acuity ≥1.0

Preoperative decimal BCVA	Eyes, no.	Postoperative 6M decimal BCVA ≥ 1.0, no (%)
≥0.9	21	12 (57)
0.7–0.8	15	7 (47)
0.5–0.6	18	8 (44)
0.3–0.4	15	2 (13)
0.1–0.2	2	0 (0)
≤0.09	2	0 (0)
Total	73	29 (40)

Notes: $P = 0.002$, Fisher's exact probability test, ≥0.5 versus <0.5; $P = 0.008$, Fisher's exact probability test, ≥0.9 versus 0.3–0.4; $P = 0.05$, Fisher's exact probability test, 0.7–0.8 versus 0.3–0.4; $P = 0.06$, Fisher's exact probability test, 0.5–0.6 versus 0.3–0.4; $P = 0.21$, Fisher's exact probability test, ≥0.9 versus 0.5–0.6; $P = 0.39$, Fisher's exact probability test, ≥0.9 versus 0.7–0.8; $P = 0.46$, Fisher's exact probability test, 0.7–0.8 versus 0.5–0.6.
Abbreviation: BCVA, best-corrected visual acuity.

decimal BCVA of 0.3–0.4 ($P = 0.008$ Fisher's exact probability test). The likelihood of obtaining a postoperative decimal BCVA ≥ 1.0 was significantly higher in eyes with a preoperative decimal BCVA ≥ 0.5 than preoperative decimal BCVA < 0.5 ($P = 0.002$, Fisher's exact probability test). In addition, there was no significant difference in the likelihood of obtaining a postoperative decimal BCVA ≥ 1.0 between preoperative decimal BCVA ≥ 0.9 and decimal BCVA of 0.7–0.8 and decimal BCVA of 0.5–0.6 (Table 3).

The associations between the preoperative FT and postoperative decimal BCVA ≥ 1.0 are shown in Table 4. The likelihood of obtaining a postoperative decimal BCVA ≥ 1.0 was 21% (6/28 eyes) in eyes with a preoperative FT of ≥400 μm, 56% (14/25 eyes) with a preoperative FT of 300 to 399 μm, 47% (9/19 eyes) with a preoperative FT of 200–299 μm, and 0% (0/1 eyes) in eyes with a preoperative FT of 100–199 μm (Table 4). The difference in the likelihood of obtaining a postoperative BCVA ≥ 1.0 for preoperative FT of 300–399 μm and 200–299 μm was

Table 4 Association between preoperative foveal thickness and postoperative decimal best-corrected visual acuity ≥1.0

Preoperative foveal thickness (μm)	Eyes, no.	Postoperative 6M decimal BCVA ≥ 1.0, no (%)
≥400	28	6 (21)
300–399	25	14 (56)
200–299	19	9 (47)
100–199	1	0 (0)
Total	73	29 (40)

Notes: $P = 0.01$, Fisher's exact probability test, ≥400 μm versus <400 μm; $P = 0.01$, Fisher's exact probability test, ≥400 μm versus 300–399 μm; $P = 0.06$, Fisher's exact probability test, ≥400 μm versus 200–299 μm; $P = 0.40$, Fisher's exact probability test, 300–399 μm versus 200–299 μm.
Abbreviation: BCVA, best-corrected visual acuity.

not significant ($P = 0.40$, Fisher's exact probability test). In addition, the likelihood of obtaining a postoperative decimal BCVA $\geq$ 1.0 in eyes with a preoperative FT of $\geq$ 400 μm was significantly lower in eyes with a preoperative FT of 300–399 μm ($P = 0.01$, Fisher's exact probability test). However, this relationship was not significant for preoperative FT of 200–299 μm ($P = 0.06$, Fisher's exact probability test). A postoperative decimal BCVA $\geq$ 1.0 was obtained in 51% (23/45 eyes) of eyes with a preoperative FT $<$ 400 μm, and the rate of obtaining a postoperative decimal BCVA $\geq$ 1.0 in eyes with a preoperative FT $<$ 400 μm was significantly higher than that in eyes with an FT $\geq$ 400 μm ($P = 0.01$, Fisher's exact probability test).

Association between preoperative findings and postoperative decimal BCVA $\geq$1.0 are shown in Table 5. The incidence of obtaining a postoperative decimal BCVA $\geq$ 1.0 was significantly higher in eyes with preoperative decimal BCVA $\geq$ 0.5 and FT $<$ 400 μm (60%) than in eyes with preoperative decimal BCVA $\geq$ 0.5 and FT $\geq$ 400 μm (20%; P = 0.03, Fisher's exact probability test) or preoperative BCVA $<$ 0.5 and FT $\geq$ 400 μm (7%; P $<$ 0.001, Fisher's exact probability test).

A summary of the clinical data of the eyes that had a postoperative decimal BCVA $\geq$ 1.0 or $<$ 1.0 is shown in Table 6. Statistical analyses on the eyes with a postoperative decimal BCVA $\geq$ 1.0 or decimal BCVA $<$ 1.0 showed that the gender, age, lens status, and surgical procedures were not significantly different in the two groups. The mean preoperative BCVA and visual improvement were 0.13 ± 0.15 and 0.18 ± 0.15 logMAR units in the postoperative decimal BCVA $\geq$ 1.0 group, whereas they were 0.30 ± 0.29 and 0.05 ± 0.23 logMAR units in the postoperative decimal BCVA $<$ 1.0 group ($P = 0.004$ and P = 0.01, Mann–Whitney U test). The mean preoperative FT was thinner in the postoperative decimal BCVA $\geq$ 1.0 group ($P = 0.07$, Mann–Whitney U test), but the difference was not significant, and the mean reduction of FT was significantly lower in the postoperative decimal BCVA $\geq$ 1.0 group than in the postoperative decimal BCVA $<$ 1.0 group ($P < 0.001$, Mann–Whitney U test). The mean preoperative FT was 344 ± 73 μm in the postoperative decimal BCVA $\geq$ 1.0 group, which was not significantly thinner than the 389 ± 121 μm in the postoperative decimal BCVA $<$ 1.0 group ($P = 0.07$, Mann–Whitney U test). However, the FT was reduced by 61 ± 35 μm in the postoperative decimal BCVA $\geq$ 1.0 group, which was significantly less than the 77 ± 48 μm in the postoperative decimal BCVA $<$ 1.0 group ($P < 0.001$, Mann–Whitney U test).

Discussion

Our results showed that 25G-TSV and membranectomy used for the treatment of idiopathic ERMs were effective in significantly improving the BCVA and reducing the FT in patients with visual disturbances including decreased BCVA or metamorphopsia. In addition, we found that the postoperative BCVA was correlated with the preoperative BCVA, preoperative FT, and postoperative FT. Approximately more than 50% of the eyes with a preoperative BCVA $\geq$ 0.5 and a preoperative FT $<$ 400 μm attained a postoperative decimal BCVA $\geq$ 1.0. Our results also demonstrated that the preoperative BCVA was significantly correlated not only with the postoperative BCVA but also with the improvement in the BCVA. Because the mean preoperative BCVA was significantly better in the postoperative decimal BCVA $\geq$ 1.0 group than in the postoperative decimal BCVA $<$ 1.0 group, a good preoperative BCVA was necessary to obtain a postoperative decimal BCVA $\geq$ 1.0, ie, a preoperative decimal BCVA

Table 5 Association between preoperative findings and postoperative decimal best-corrected visual acuity $\geq$1.0

Group	Preoperative findings	Eyes, no.	Postoperative 6M decimal BCVA $\geq$ 1.0, no (%)
1	Decimal BCVA $\geq$ 0.5 and FT $<$ 400	40	24 (60)
2	Decimal BCVA $\geq$ 0.5 and FT $\geq$400	10	2 (20)
3	Decimal BCVA $<$ 0.5 and FT $<$ 400	8	2 (25)
4	Decimal BCVA $<$ 0.5 and FT $\geq$400	15	1 (7)
	Total	73	29 (40)

$P = 0.03$, Fisher's exact probability test, Group 1 versus Group 2.

$P = 0.08$, Fisher's exact probability test, Group 1 versus Group 3.

$P < 0.001$, Fisher's exact probability test, Group 1 versus Group 4.

$P = 0.62$, Fisher's exact probability test, Group 2 versus Group 3.

$P = 0.35$, Fisher's exact probability test, Group 2 versus Group 4.

$P = 0.27$, Fisher's exact probability test, Group 3 versus Group 4.

Abbreviations: BCVA = best-corrected visual acuity; FT = foveal thickness (μm).

Table 6 Summary of clinical data by postoperative decimal best-corrected visual acuity ≥1.0 or <1.0

	Postoperative decimal BCVA ≥ 1.0	Postoperative decimal BCVA < 1.0	*P* value
No. eyes	29	44	
No. patients	29	44	
Gender (no./%)			0.08*
Male	13 (45)	11 (25)	
Female	16 (55)	33 (75)	
Age (yrs)			
Mean ± SD	65.9 ± 12.8	68.1 ± 8.5	0.57#
Median	68	67	
Range	27–87	50–82	
Lens status (baseline; no./%)			0.69*
Phakic	24 (83)	37 (84)	
Pseudophakic	5 (17)	7 (16)	
Surgical procedure (no./%)			0.35*
25G-TSV	14 (48)	18 (36)	
Triple surgery	15 (52)	26 (64)	
Decimal BCVA (mean)			
Baseline	0.74	0.50	
Postoperative 6M	1.10	0.56	
BCVA (logMAR; mean ± SD)			
Baseline	0.13 ± 0.15	0.30 ± 0.29	0.004#
Postoperative 6M	−0.04 ± 0.07	0.25 ± 0.29	<0.001#
Improvement	0.18 ± 0.15	0.05 ± 0.23	0.01#
Foveal thickness (μm; mean ± SD)			
Baseline	344 ± 73	389 ± 121	0.07#
Postoperative 6M	283 ± 39	312 ± 78	0.11#
Reduction	61 ± 35	77 ± 48	<0.001#

Notes: *Fisher's exact probability test; #Mann–Whitney test. Triple surgery, phacoemulsification and aspiration, intraocular lens implant, and 25-gauge transconjunctival sutureless vitrectomy.

Abbreviations: SD, standard deviation; 25G-TSV, 25-gauge transconjunctival sutureless vitrectomy; BCVA, best-corrected visual acuity; logMAR, logarithm of the minimum angle of resolution.

of ≥ 0.5. Our findings indicated that the reduction of the FT was significantly lower in the postoperative decimal BCVA ≥ 1.0 group, which was also reasonable because the reduction of FT was significantly correlated with preoperative BCVA (logMAR). On the other hand, although eyes with good preoperative BCVA showed a decreased likelihood of visual improvements, the improvement of the BCVA was significantly higher in the postoperative decimal BCVA ≥ 1.0 group than in the postoperative decimal BCVA < 1.0 group. The reason for this is unclear. However, the status of the photoreceptor inner and outer segment (IS/OS) or external limiting membrane (ELM) might be one of the explanations for this. The use of a spectral domain OCT would have helped in evaluating the photoreceptor integrity in more detail.

A postoperative decimal BCVA ≥ 1.0 also correlated with a preoperative FT of <400 μm. We suggest that because the preoperative FT was significantly correlated with the preoperative BCVA and the postoperative BCVA, the postoperative BCVA was worse in eyes with thicker preoperative FT. If the preoperative FT was ≥ 400 μm, the preoperative decimal BCVA might be too low to attain a postoperative decimal BCVA ≥ 1.0, even if the visual improvement was high. Thus, if the effects of the ERM had progressed to cause a lower decimal BCVA and thicker FT, the postoperative visual recovery of decimal BCVA ≥ 1.0 would not be expected, in spite of a larger FT reduction and improvement in BCVA. We conclude that the eyes with both preoperative FT < 400 μm and preoperative decimal BCVA ≥ 0.5 were the best candidates to obtain a postoperative decimal BCVA of ≥1.0 postoperatively.

The improvement of the BCVA and reduction of the FT following surgery have been reported in the literature.[7,13–16] Several studies have reported that the preoperative FT was significantly correlated with the preoperative BCVA, but the postoperative FT was not significantly correlated with the postoperative BCVA.[15,17,18] However, a study by Suh et al reported that the postoperative FT was significantly correlated with the postoperative BCVA after ERM surgery, which is similar to our study.[19] Discrepancies in the association of the postoperative BCVA and FT in earlier studies are probably

due to different surgical procedures and low uniformity of various interventions, including ILM removal, dye used, and vitrectomy instruments (20 gauge or 25 gauge). If the ILM was completely removed as in the study by Shimada et al and this study, the residual ILM might not influence the postoperative macular surface to worsen the FT and BCVA.[20]

The removal of the ILM is still controversial because electrophysiological studies have shown some retinal dysfunction following ILM removal and because the use of dye had some retinal toxicity.[21,22] However, studies have shown a decrease in the recurrences of ERM after ILM peeling and improvement of the BCVA and FT.[20,23–25] Our results showed a 1.4% (1/73 eyes) recurrence rate after more than a mean postoperative period of 9 months.

Because the IS/OS were not evaluated in the study presented, there have been two recent reports that discussed the association between the preoperative OCT images of the IS/OS junction of the photoreceptors and the visual outcomes after ERM surgery.[17,19] We did not study the IS/OS junction as a prognostic factor because we were not able to precisely detect it because of the low resolution of the OCT we used. In addition, the IS/OS junction is difficult to detect when the FT is thick. Although it is more difficult to detect the ELM by low-resolution OCT, we believe that the BCVA in eyes with ERM would be correlated also with the status of ELM if it could be detected.[26,27] However, because our results showed that eyes with postoperative decimal BCVA $\geq$ 1.0 had good preoperative BCVA, and because the nonoperated ERM eyes with photoreceptor defects have significantly lower visual acuity,[28] all of our cases that had a postoperative BCVA $\geq$ 1.0 probably had a distinct IS/OS junction and ELM in the fovea. Thus, we believe that the preoperative BCVA and FT could be prognostic parameters for all ophthalmologists without knowing precisely the status of the IS/OS junction and even an ELM.

The duration of symptoms was not studied as a prognostic factor[28,29] because the exact onset of the ERM, especially if the patients had good BCVA, is uncertain.

There are limitations of our study, including its retrospective nature, short follow-up period, small number of patients, and use of time-domain OCT. In addition, although a final decimal BCVA of 1.0 is only one aspect of the visual benefit in ERM surgery, and the degree of visual improvement and reduction of metamorphopsia are also important benefits of this surgery, the aim of this study was to identify factors that led to a postoperative decimal BCVA $\geq$ 1.0. Nevertheless, our findings indicate that surgery with 25G-TSV/membranectomy for idiopathic ERM is a useful method to obtain good decimal BCVA $\geq$ 1.0 postoperatively. Based on our study results, a postoperative decimal BCVA of $\geq$ 1.0 can be achieved in patients whose preoperative decimal BCVA has not deteriorated beyond 0.5 and whose central macular thickness has not exceeded 400 µm. However, many patients in this range of vision and FT are asymptomatic, and we should remember that all surgery carries inherent risks.

In conclusion, our findings indicate that eyes with both preoperative BCVA $\geq$ 0.5 and FT $<$ 400 µm have a significantly better chance of obtaining a postoperative decimal BCVA $\geq$ 1.0 following removal of the idiopathic ERM.

Note

We thank Dr. Masahiko Shimura (Department of Ophthalmology, NTT East Japan Tohoku Hospital) for the critical comments on the manuscript. Parts of this paper were presented at the Annual Meeting of the Japanese Society of Clinical Ophthalmology, Fukuoka, Japan, in October 2009. This work was supported in part by research grants from the Ministry of Education, Culture, Sports, Science and Technology, Tokyo, Japan.

Disclosure

The authors report no conflicts of interest in this work.

References

1. Haas A, Seidel G, Steinbrugger I, et al. Twenty-three-gauge and 20-gauge vitrectomy in epiretinal membrane surgery. *Retina*. 2010;30:112–116.
2. Rizzo S, Belting C, Genovesi-Ebert F, di Bartolo E. Incidence of retinal detachment after small-incision, sutureless pars plana vitrectomy compared with conventional 20-gauge vitrectomy in macular hole and epiretinal membrane surgery. *Retina*. 2010;30:1065–1071.
3. Kunimoto DY, Kaiser RS. Incidence of endophthalmitis after 20- and 25-gauge vitrectomy. *Ophthalmology*. 2007;114:2133–2137.
4. Michels RG. Vitreous surgery for macular pucker. *Am J Ophthalmol*. 1981;92:628–639.
5. Michels RG. Vitrectomy for macular pucker. *Ophthalmology*. 1984;91:1384–1388.
6. Hasegawa T, Emi K, Ikeda T, Watanabe M, Takaoka G. Long-term prognosis of internal limiting membrane peeling for idiopathic epiretinal membrane. *Nippon Ganka Gakkai Zasshi*. 2004;108:150–156.
7. Ishida M, Takeuchi S, Nakamura M, Morimoto K, Okisaka S. The surgical outcome of vitrectomy for idiopathic epiretinal membranes and foveal thickness before and after surgery. *Nippon Ganka Gakkai Zasshi*. 2004;108:18–22.
8. Fujii GY, de Juan E Jr, Humayun MS, et al. A new 25-gauge instrument system for transconjunctival sutureless vitrectomy surgery. *Ophthalmology*. 2002;109:1807–1812; discussion 1813.
9. Fujii GY, de Juan E Jr, Humayun MS, et al. Initial experience using the transconjunctival sutureless vitrectomy system for vitreoretinal surgery. *Ophthalmology*. 2002;109:1814–1820.

10. Kadonosono K, Yamakawa T, Uchio E, Yanagi Y, Tamaki Y, Araie M. Comparison of visual function after epiretinal membrane removal by 20-gauge and 25-gauge vitrectomy. *Am J Ophthalmol*. 2006;142:513–515.
11. Okamoto F, Okamoto C, Sakata N, et al. Changes in corneal topography after 25-gauge transconjunctival sutureless vitrectomy versus after 20-gauge standard vitrectomy. *Ophthalmology*. 2007;114:2138–2141.
12. Oshima Y, Kadonosono K, Yamaji H, et al. Multicenter survey with a systematic overview of acute-onset endophthalmitis after transconjunctival microincision vitrectomy surgery. *Am J Ophthalmol*. 2010;150:716–725.e1.
13. Niwa T, Terasaki H, Kondo M, Piao CH, Suzuki T, Miyake Y. Function and morphology of macula before and after removal of idiopathic epiretinal membrane. *Invest Ophthalmol Vis Sci*. 2003;44:1652–1656.
14. Lee JW, Kim IT. Outcomes of idiopathic macular epiretinal membrane removal with and without internal limiting membrane peeling: a comparative study. *Jpn J Ophthalmol*. 2010;54:129–134.
15. Koutsandrea CN, Apostolopoulos MN, Alonistiotis DA, et al. Indocyanine green-assisted epiretinal membrane peeling evaluated by optical coherence tomography and multifocal electroretinography. *Clin Ophthalmol*. 2007;1:535–544.
16. Hillenkamp J, Saikia P, Gora F, et al. Macular function and morphology after peeling of idiopathic epiretinal membrane with and without the assistance of indocyanine green. *Br J Ophthalmol*. 2005;89:437–443.
17. Mitamura Y, Hirano K, Baba T, Yamamoto S. Correlation of visual recovery with presence of photoreceptor inner/outer segment junction in optical coherence images after epiretinal membrane surgery. *Br J Ophthalmol*. 2009;93:171–175.
18. Massin P, Allouch C, Haouchine B, et al. Optical coherence tomography of idiopathic macular epiretinal membranes before and after surgery. *Am J Ophthalmol*. 2000;130:732–739.
19. Suh MH, Seo JM, Park KH, Yu HG. Associations between macular findings by optical coherence tomography and visual outcomes after epiretinal membrane removal. *Am J Ophthalmol*. 2009;147:473–480.e3.
20. Shimada H, Nakashizuka H, Hattori T, Mori R, Mizutani Y, Yuzawa M. Double staining with brilliant blue G and double peeling for epiretinal membranes. *Ophthalmology*. 2009;116:1370–1376.
21. Terasaki H, Miyake Y, Nomura R, et al. Focal macular ERGs in eyes after removal of macular ILM during macular hole surgery. *Invest Ophthalmol Vis Sci*. 2001;42:229–234.
22. Ueno S, Kondo M, Piao CH, Ikenoya K, Miyake Y, Terasaki H. Selective amplitude reduction of the PhNR after macular hole surgery: ganglion cell damage related to ICG-assisted ILM peeling and gas tamponade. *Invest Ophthalmol Vis Sci*. 2006;47:3545–3549.
23. Kwok A, Lai TY, Yuen KS. Epiretinal membrane surgery with or without internal limiting membrane peeling. *Clin Experiment Ophthalmol*. 2005;33:379–385.
24. Kwok AK, Lai TY, Li WW, Woo DC, Chan NR. Indocyanine green-assisted internal limiting membrane removal in epiretinal membrane surgery: a clinical and histologic study. *Am J Ophthalmol*. 2004;138:194–199.
25. Park DW, Dugel PU, Garda J, et al. Macular pucker removal with and without internal limiting membrane peeling: pilot study. *Ophthalmology*. 2003;110:62–64.
26. Wakabayashi T, Fujiwara M, Sakaguchi H, Kusaka S, Oshima Y. Foveal microstructure and visual acuity in surgically closed macular holes: spectral-domain optical coherence tomographic analysis. *Ophthalmology*. 2010;117:1815–1824.
27. Wakabayashi T, Oshima Y, Fujimoto H, et al. Foveal microstructure and visual acuity after retinal detachment repair: imaging analysis by Fourier-domain optical coherence tomography. *Ophthalmology*. 2009;116:519–528.
28. Michalewski J, Michalewska Z, Cisiecki S, Nawrocki J. Morphologically functional correlations of macular pathology connected with epiretinal membrane formation in spectral optical coherence tomography (SOCT). *Graefes Arch Clin Exp Ophthalmol*. 2007;245:1623–1631.
29. Pesin SR, Olk RJ, Grand MG, et al. Vitrectomy for premacular fibroplasia. Prognostic factors, long-term follow-up, and time course of visual improvement. *Ophthalmology*. 1991;98:1109–1114.

EURETINA – Original Paper

Ophthalmologica

Ophthalmologica 2011;226:198–204
DOI: 10.1159/000330745

Received: December 17, 2010
Accepted after revision: July 10, 2011
Published online: September 2, 2011

Difficulty in Inserting 25- and 23-Gauge Trocar Cannula during Vitrectomy

Hiroshi Kunikata[a] Fumihiko Nitta[a] Yasuhiko Meguro[a] Naoko Aizawa[a]
Takehiro Hariya[a] Naoki Chiba[a] Toshiaki Abe[b] Kohji Nishida[a, c]

[a]Department of Ophthalmology and Visual Science and [b]Division of Clinical Cell Therapy, Tohoku University Graduate School of Medicine, Sendai, and [c]Department of Ophthalmology, Osaka University Medical School, Suita, Japan

Key Words
Retinal detachment · 25-gauge vitrectomy · 23-gauge vitrectomy · Choroidal detachment · Trocal cannula

Abstract
Purpose: To determine the incidence of difficulty in inserting a 25- and 23-gauge trocar cannula (DITC) during 25- or 23-gauge micro-incision vitrectomy surgery (MIVS). ***Methods:*** Retrospective, consecutive, interventional case series performed by a single surgeon at a single centre. We defined a DITC as the condition where at least 1 trocar cannula could not be inserted into the vitreous at the beginning of MIVS. The incidence of DITC was calculated from 1,525 eyes, and the pre-operative demographics of the DITC cases were compared to those of the non-DITC cases. ***Results:*** The incidence of DITC for all cases was 0.6% (9 of 1,525 eyes). Overall, there were 242 eyes with a retinal detachment (RD), and 8 of the 9 eyes with DITC had an RD with an incidence of 3.3% (8 of 242 RD eyes). Seven of these 8 eyes had a total RD, 4 also had a choroidal detachment, 4 eyes were also myopic (>–8.0 dpt, high myopia), and 6 of the 8 eyes were hypotonic (<8 mm Hg). The DITC cases had larger RDs ($p < 0.0001$), a higher incidence of choroidal detachment ($p < 0.0001$), higher myopia ($p = 0.0204$) and hypotony ($p = 0.0003$) than the non-DITC eyes with an RD. ***Conclusions:*** A large RD, a choroidal detachment, high myopia and hypotony are significant risk factors for DITC. We recommend that MIVS should be performed cautiously for eyes with these risk factors.

Introduction

Twenty-five- and 23-gauge micro-incision vitrectomy surgery (MIVS) were first reported in 2002 and 2005, respectively. These techniques have become commonly used throughout the world [1–5]. The indications for MIVS for different kinds of vitreoretinal diseases including primary rhegmatogenous retinal detachment (RD) have increased [1, 6, 7].

This paper was partially presented at the Annual Meeting of the Japanese Retina and Vitreous Society, Nagoya, December 2009.

KARGER

Fax +41 61 306 12 34
E-Mail karger@karger.ch
www.karger.com

0030–3755/11/2264–0198$38.00/0

Accessible online at:
www.karger.com/oph

Hiroshi Kunikata, MD, PhD
Department of Ophthalmology and Visual Science
Tohoku University Graduate School of Medicine
1-1 Seiryo-machi, Aoba-ku, Sendai 980-8574 (Japan)
Tel. +81 22 717 7294, E-Mail kunikata@oph.med.tohoku.ac.jp